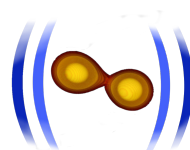




FRIEDRICH-SCHILLER-
UNIVERSITÄT
JENA



European Research Council
Established by the European Commission



www.computational-relativity.org

Modeling matter and eccentricity effects in compact binary mergers

TEOBResumS: https://bitbucket.org/eob_ihes/teobresums/src/master/

NR waveforms: https://core-gitlfs.tpi.uni-jena.de/core_database

bajes: <https://github.com/matteobreschi/bajes>

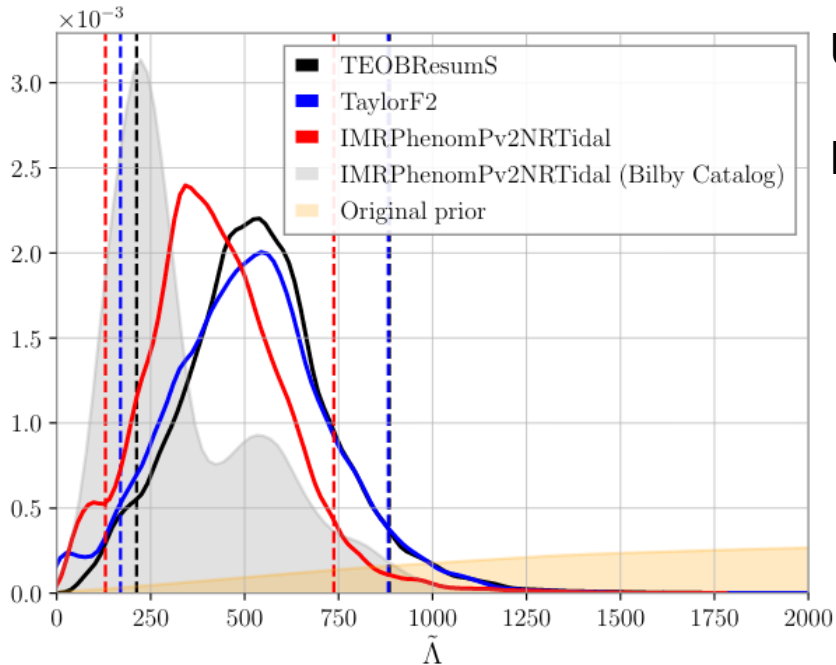
S. Bernuzzi

KITP “High-Precision Gravitational Waves” April 2022

Tidal (and matter) effects

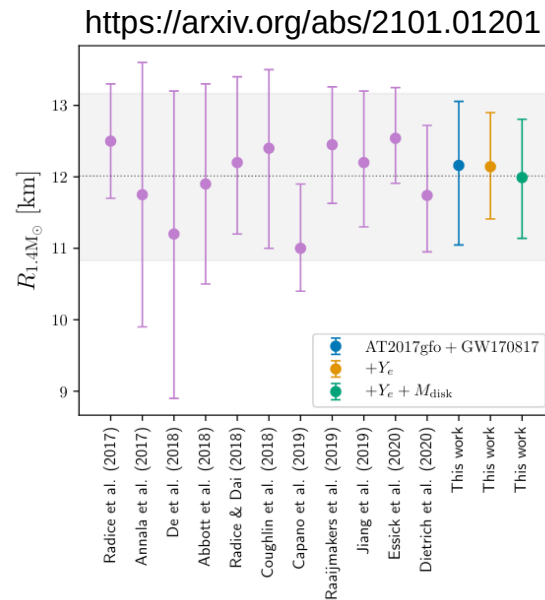
Tidal parameters inference & wvf systematics

Gamba, Breschi, SB+ [<https://arxiv.org/abs/2009.08467>]



Updated NS radius measurement:

$$R_{1.4} = 12.5^{+1.1}_{-1.8} \text{ km}$$



GW170817: no significant wvf systematics BUT $\bar{\Lambda}$ “double peaked” posteriors ...

1kHz cut-off removes double peaks, less wvf biases and shifts to larger $\bar{\Lambda}$ (larger radii) for comparable log-like.

Estimated <10% SNR above $f > 1\text{kHz}$; high-frequencies issues in $\bar{\Lambda}$ -inference? (Dai+ 2018, Narikawa+ 2019)

Main challenge

PHYSICAL REVIEW D **85**, 123007 (2012)

Measurability of the tidal polarizability of neutron stars in late-inspiral gravitational-wave signals

Thibault Damour and Alessandro Nagar

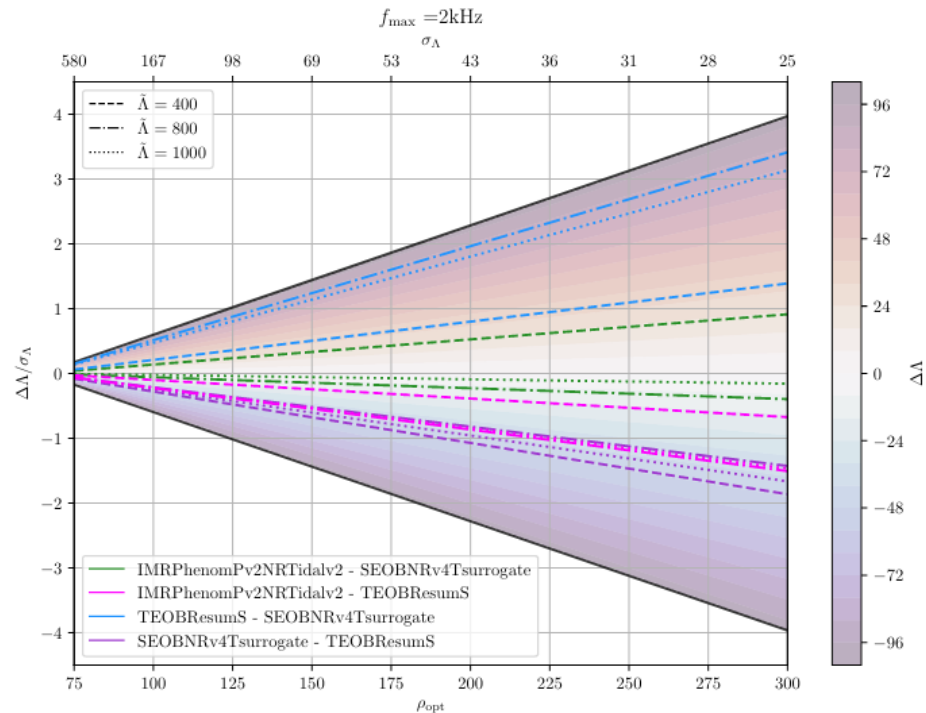
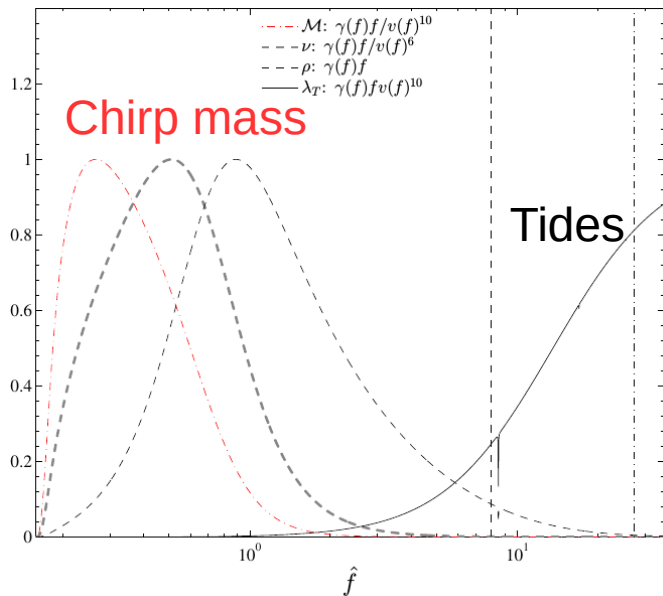
Institut des Hautes Etudes Scientifiques, 91440 Bures-sur-Yvette, France ICRA.Net, 65122 Pescara, Italy

Loïc Villain

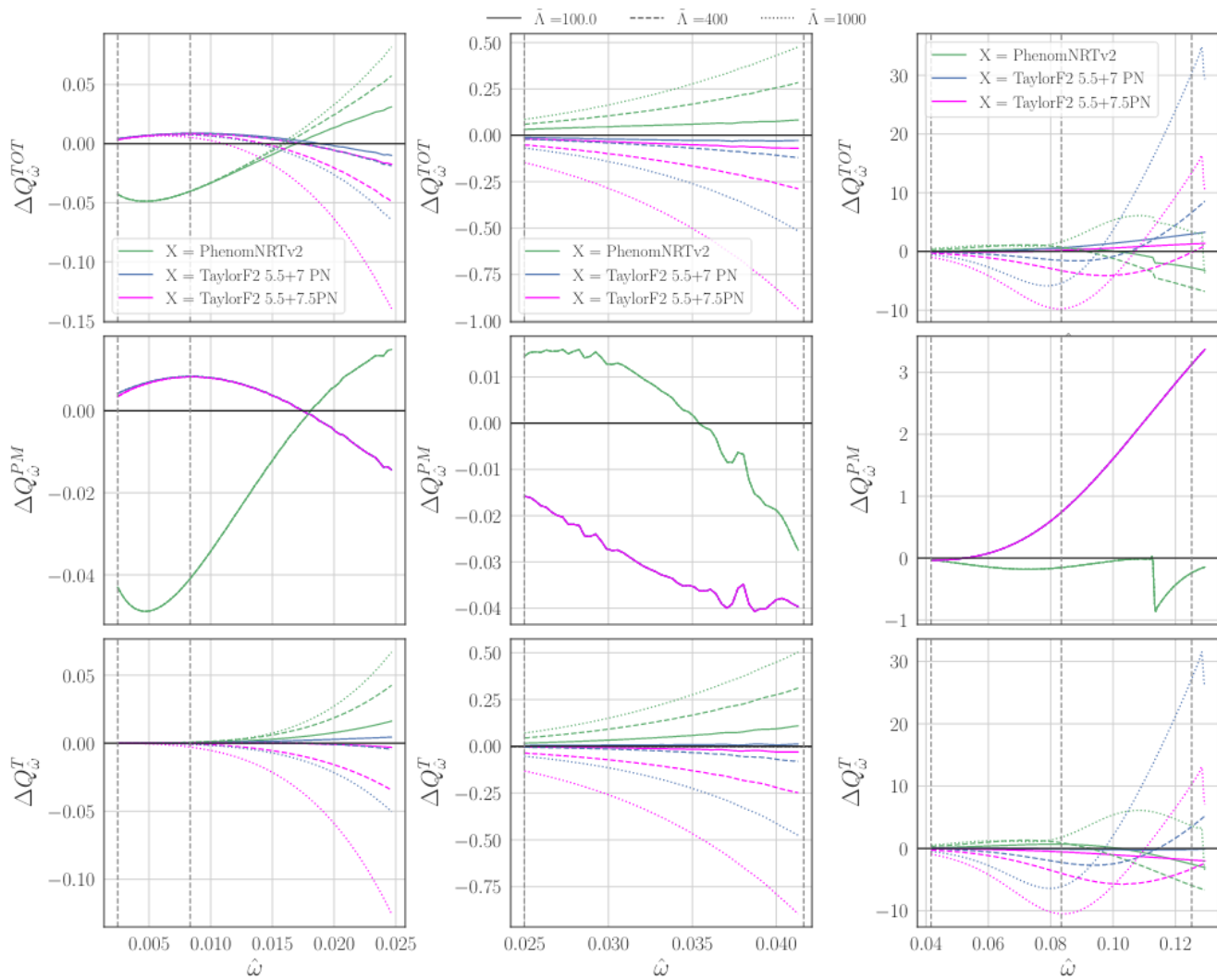
Laboratoire de Mathématiques et de Physique Théorique, Univ. F. Rabelais—CNRS (UMR 7350),

Féd. Denis Poisson, 37200 Tours, France

(Received 20 March 2012; published 15 June 2012)

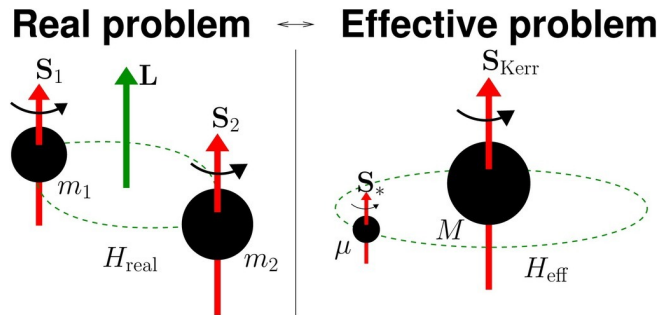


[Gamba, Breschi, SB+ <https://arxiv.org/abs/2009.08467>]



Effective-one-body framework in a nutshell

[Buonanno&Damour PRD 2000a, 2000b]



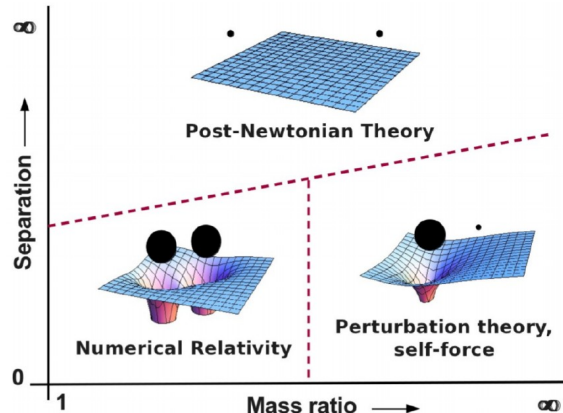
$$H_{\text{eff}} \sim \mu \sqrt{A(u)(1 + p_\phi^2 u^2) + p_r^{2*}}$$

$$A(u; \nu; \kappa_2^T) = A^0(u; \nu) + A^T(u; \nu; \kappa_2^T)$$

$$A^0(u; \nu) = 1 - 2u + \nu(\dots)$$

Credit: A. Taracchini

Factorized (resummed) PN waveform [Damour,Iyer,Nagar 2008]
 Includes test-mass limit (i.e. particle on Schwarzschild)
 Includes post-Newtonian and self-force results
 Uses resummation techniques → predictive strong-field regime
 Includes tidal interactions (→ BNS) [Damour&Nagar PRD 2010]
 Flexible framework → NR informed



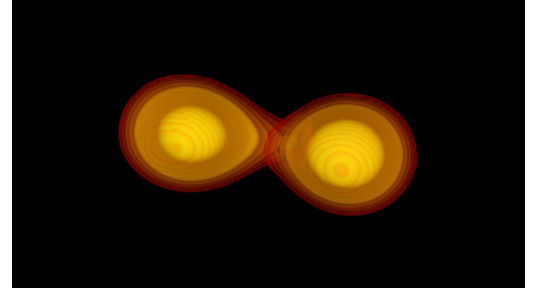
Credit: L. Barak

Effective one body description of tidal effects in inspiralling compact binaries

Thibault Damour and Alessandro Nagar

Institut des Hautes Etudes Scientifiques, 91440 Bures-sur-Yvette, France and ICRA/Net, 65122 Pescara, Italy
(Received 26 November 2009; published 8 April 2010)

$$\kappa_2^T = 2 \left[\frac{X_A}{X_B} \left(\frac{X_A}{C_A} \right)^5 k_2^A + \frac{X_B}{X_A} \left(\frac{X_B}{C_B} \right)^5 k_2^B \right]$$



Tidal coupling constant (Analogous to the reduced tidal parameter $\bar{\Lambda}$ [Favata 2013])

Hamiltonian
(Newtonian limit):

$$H_{\text{EOB}} \approx Mc^2 + \frac{\mu}{2} (\mathbf{p}^2 + A(r) - 1)$$

$$A(r) = 1 - \frac{2}{r} - \frac{\kappa_2^T (k_2)}{r^6}$$

Waveform:

$$h \sim A f^{-7/6} e^{-i\Psi(x(f))} = A f^{-7/6} e^{-i\Psi_{\text{pp}}(x) + i39/4 \kappa_2^T x^{5/2}}$$

Modeling the Dynamics of Tidally Interacting Binary Neutron Stars up to the Merger

Sebastiano Bernuzzi,^{1,2} Alessandro Nagar,³ Tim Dietrich,⁴ and Thibault Damour³

¹TAPIR, California Institute of Technology, Pasadena, California 91125-0001, USA

²DiFeST, University of Parma, I-43124 Parma, Italy

³Institut des Hautes Etudes Scientifiques, 91440 Bures-sur-Yvette, France

⁴Theoretical Physics Institute, University of Jena, 07743 Jena, Germany

(Received 15 December 2014; revised manuscript received 18 February 2015; published 23 April 2015)

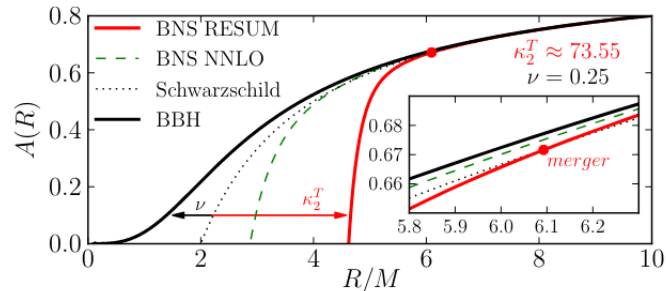
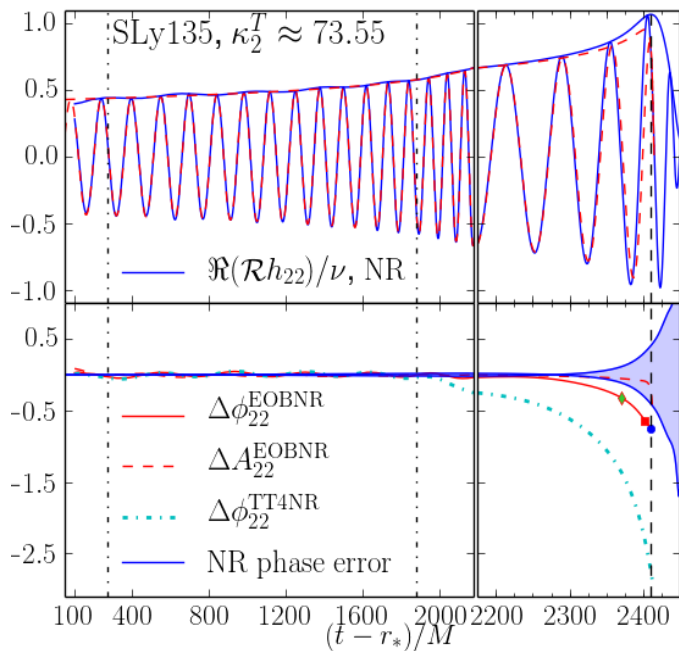


FIG. 1: The main radial gravitational potential $A(R)$ in various EOB models. Finite-mass ratio effects (ν) make the gravitational interaction less attractive than the Schwarzschild relativistic potential $A_{\text{Schw}} = 1 - 2M/R$, while tides (κ_2^T , see Table I) make it more attractive (especially at short separations).

PHYSICAL REVIEW D **90**, 124037 (2014)

Gravitational self-force corrections to two-body tidal interactions and the effective one-body formalism

Donato Bini¹ and Thibault Damour²

¹Istituto per le Applicazioni del Calcolo “M. Picone,” CNR, I-00185 Rome, Italy

²Institut des Hautes Etudes Scientifiques, 91440 Bures-sur-Yvette, France

(Received 24 September 2014; published 10 December 2014)

See also Bini, Damour, Feye 2013, Dolan+ 2014
 Akcay, SB+ [<https://arxiv.org/abs/1812.02744>]

Dynamical Tides in General Relativity: Effective Action and Effective-One-Body Hamiltonian

Jan Steinhoff,^{1,2} Tanja Hinderer,^{3,1} Alessandra Buonanno,^{1,3} and Andrea Taracchini¹

¹Max Planck Institute for Gravitational Physics (Albert Einstein Institute), Am Mühlenberg 1, Potsdam 14476, Germany

²Centro Multidisciplinar de Astrofísica — CENTRA, Departamento de Física, Instituto Superior Técnico — IST, Universidade de Lisboa — ULisboa, Avenida Rovisco Pais 1, 1049-001 Lisboa, Portugal

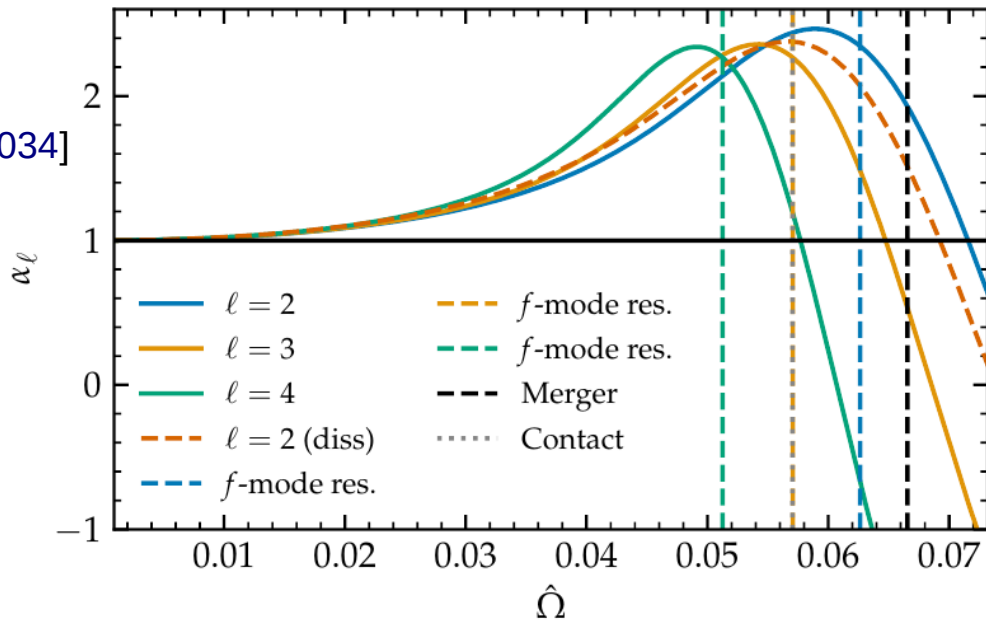
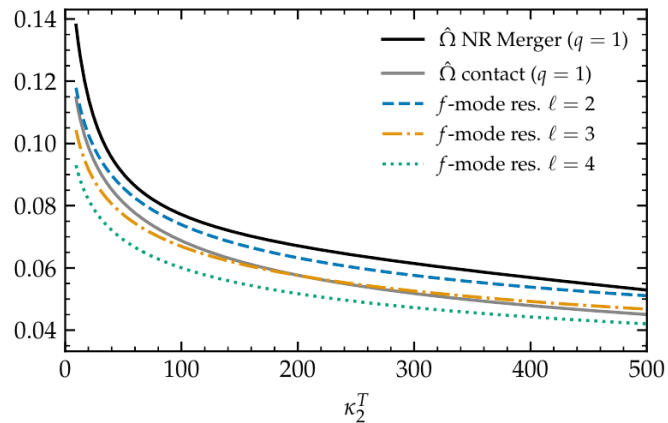
³Department of Physics, University of Maryland, College Park, MD 20742, USA

(Dated: November 17, 2016)

See also

Lai [<https://arxiv.org/abs/astro-ph/9404062>]

Kokkotas&Schaefer [<https://arxiv.org/abs/gr-qc/9502034>]



Closed-form tidal approximants for binary neutron star gravitational waveforms constructed from high-resolution numerical relativity simulations

Tim Dietrich¹, Sebastiano Bernuzzi^{2,3}, and Wolfgang Tichy⁴

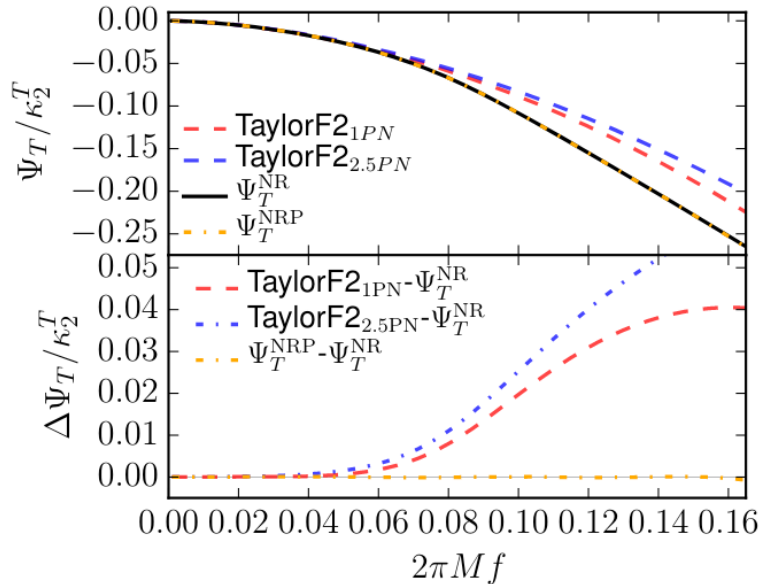


FIG. 3. Frequency-domain tidal approximants. Top panel shows $\Psi_T/\kappa_{\text{eff}}^T$ as given by the TaylorF2_{1PN}, TaylorF2_{2.5PN} [32], Eq. (6), and Eq. (7). Bottom panel: Difference between the frequency-domain representations.

$$\phi(\hat{\omega}) \approx \phi_0(\hat{\omega}) + \phi_{SO}(\hat{\omega}) + \phi_T(\hat{\omega})$$

$$\frac{d^2\Psi_T^{\text{SPA}}}{d\omega_f^2} = \frac{Q_\omega(\omega_f)}{\omega_f^2}$$

$$\Psi_T^{\text{NRP}} = -\kappa_{\text{eff}}^T \frac{\tilde{c}_{\text{Newt}}}{X_A X_B} x^{5/2} \times \frac{1 + \tilde{n}_1 x + \tilde{n}_{3/2} x^{3/2} + \tilde{n}_2 x^2 + \tilde{n}_{5/2} x^{5/2}}{1 + \tilde{d}_1 x + \tilde{d}_{3/2} x^{3/2}}$$

Accuracy of NR waveforms

TABLE V. Faithfulness values \mathcal{F} computed considering frequencies from f_{low} to f_{mrg} between simulations with the same intrinsic parameters and two different resolutions, extracted at $r/M = 1000$. The source is situated in the same sky location as GW170817, and the waveform polarizations h_+ and h_\times are computed and projected on the Livingston detector. We employ the `aLIGODesignSensitivityP1200087` [22] PSD from `pycbc` [110] to compute the matches, and compare the values obtained to the thresholds \mathcal{F}_{thr} calculated with Eq. 19 with $\epsilon^2 = 1$ or $\epsilon^2 = N$. A tick \checkmark indicates that $\mathcal{F} > \mathcal{F}_{\text{thr}}$. Conversely, a cross \times indicates that $\mathcal{F} < \mathcal{F}_{\text{thr}}$.

Sim	r ^a	\mathcal{F}	SNR						
			14		30		80		
			$N = 6$	1	$N = 6$	1	$N = 6$	1	
BAM:0011	[96, 64]	0.991298	\checkmark	\times	\times	\times	\times	\times	\times
BAM:0017	[96, 64]	0.985917	\checkmark	\times	\times	\times	\times	\times	\times
BAM:0021	[96, 64]	0.957098	\times	\times	\times	\times	\times	\times	\times
BAM:0037	[216, 144]	0.998790	\checkmark	\checkmark	\checkmark	\times	\times	\times	\times
BAM:0048	[108, 72]	0.983724	\times	\times	\times	\times	\times	\times	\times
BAM:0058	[64, 64]	0.999127	\checkmark	\checkmark	\checkmark	\times	\times	\times	\times
BAM:0064	[240, 160]	0.997427	\checkmark	\times	\checkmark	\times	\times	\times	\times
BAM:0091	[144, 108]	0.997810	\checkmark	\checkmark	\checkmark	\times	\times	\times	\times
BAM:0094	[144, 108]	0.996804	\checkmark	\times	\checkmark	\times	\times	\times	\times
BAM:0095	[256, 192]	0.999550	\checkmark	\checkmark	\checkmark	\checkmark	\checkmark	\checkmark	\times
BAM:0107	[128, 96]	0.995219	\checkmark	\times	\times	\times	\times	\times	\times
BAM:0127	[128, 96]	0.999011	\checkmark	\checkmark	\checkmark	\times	\times	\times	\times

^a Number of grid point (linear resolution) of the finest grid refinement, roughly covering the diameter of one NS

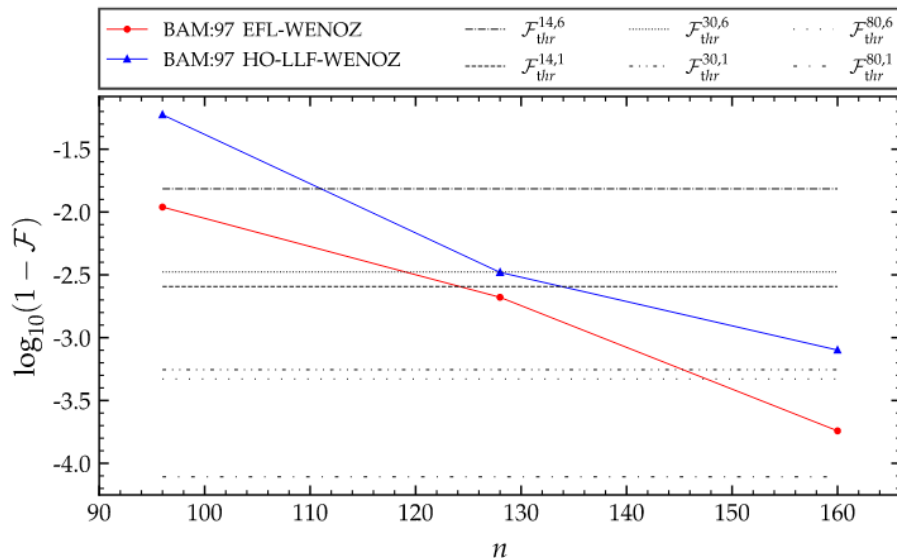
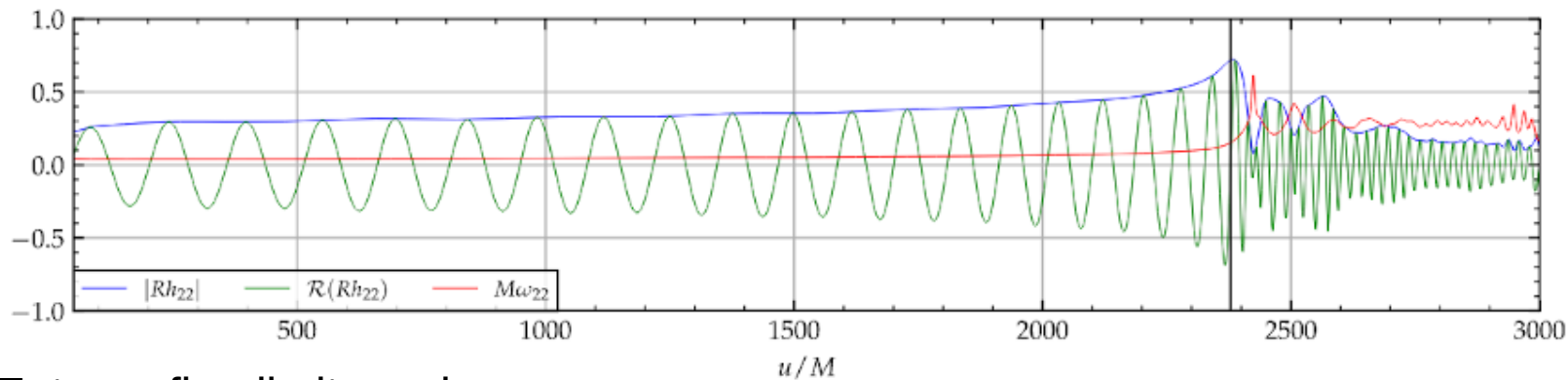
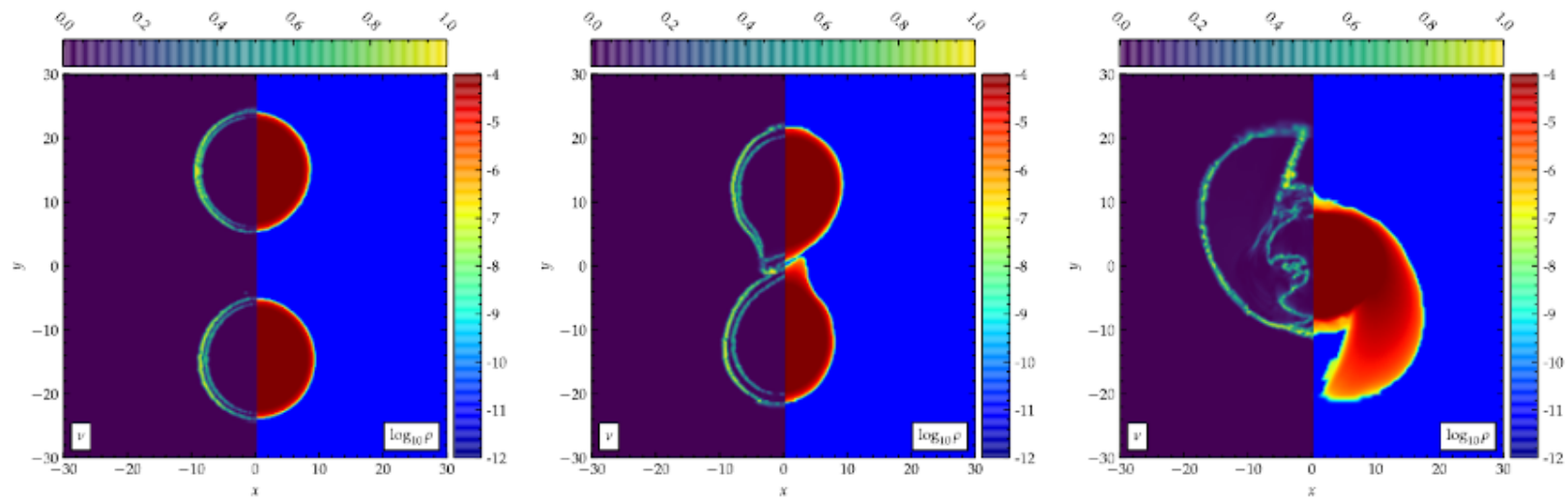


FIG. 21. Faithfulness as a function of the resolution for the BAM:97 simulation.

Doulis, Atteneder, SB, Bruegmann
[\[https://arxiv.org/abs/2202.08839\]](https://arxiv.org/abs/2202.08839)



Entropy flux-limiter scheme

Doulis, Atteneder, SB, Bruegmann [<https://arxiv.org/abs/2202.08839>]

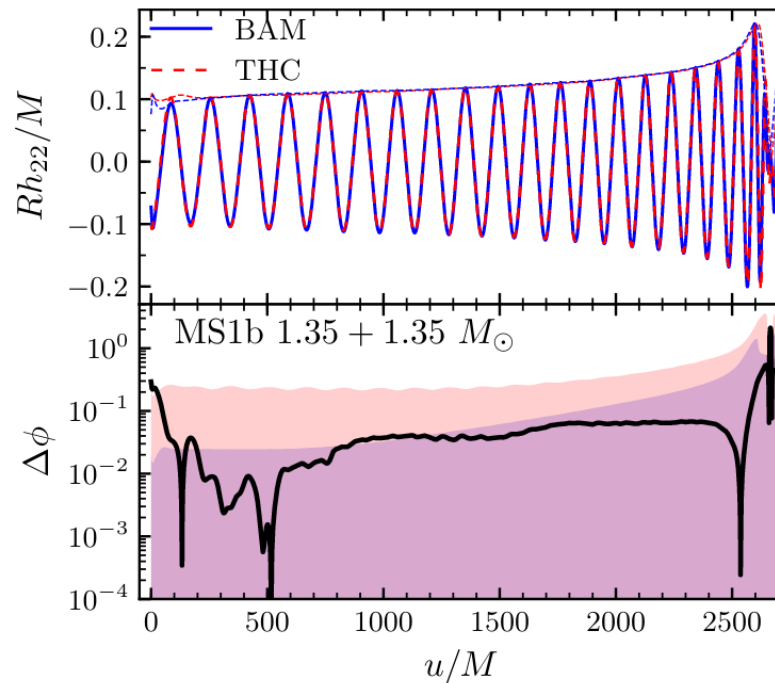
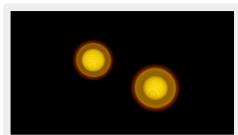
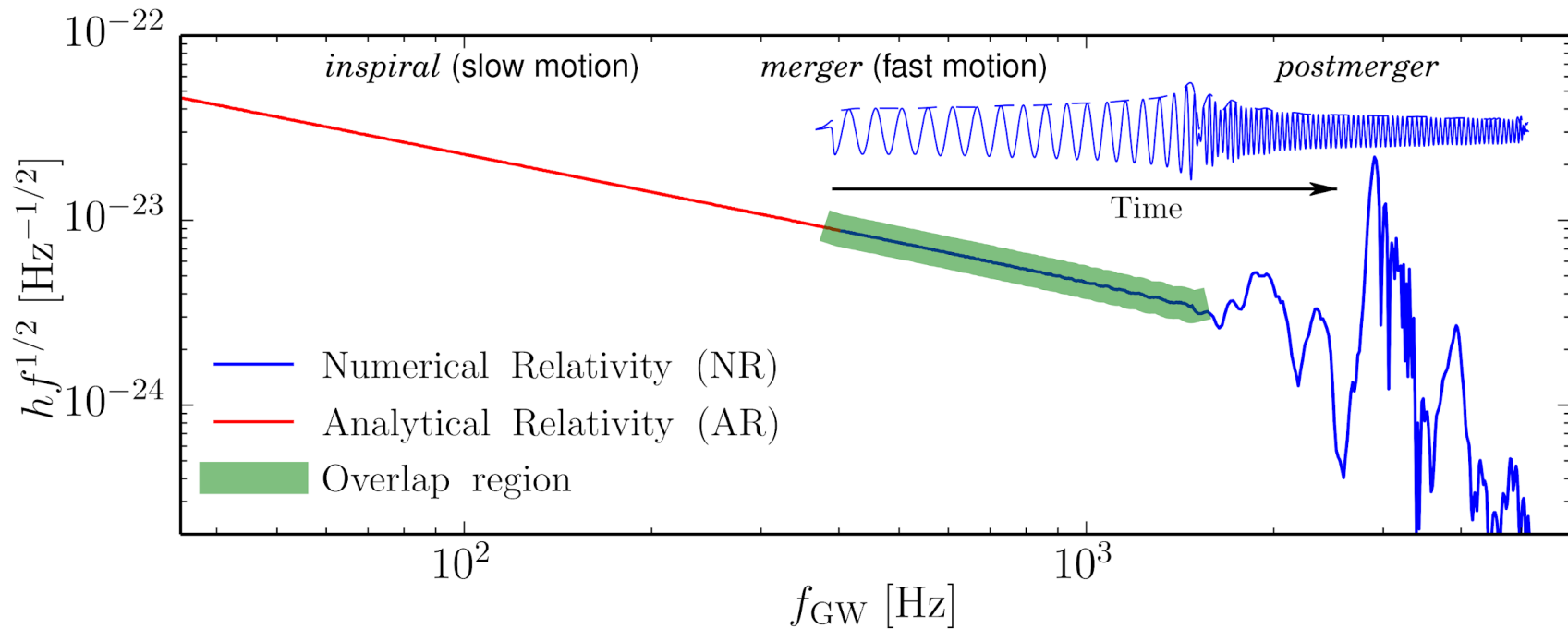
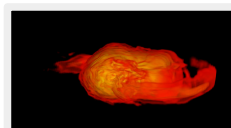
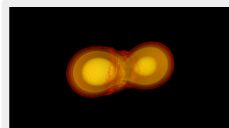


FIG. 31. Systematic uncertainties in BNS numerical relativity inspiral-merger waveform. Waveforms from two independent and high-order codes are compared.

The BNS gravitational-wave spectrum



SB+ <https://arxiv.org/abs/1504.01764>
Breschi, SB+ <https://arxiv.org/abs/1908.11418>



GW constraints on NS extreme matter

Full-spectrum (mock) analysis using ET (minimum SNR threshold for a PM detection)
 NS maximum density to 15% and maximum mass to 12% (90% conf. Lev.)

[Breschi, SB+ <https://arxiv.org/abs/2110.06957>]

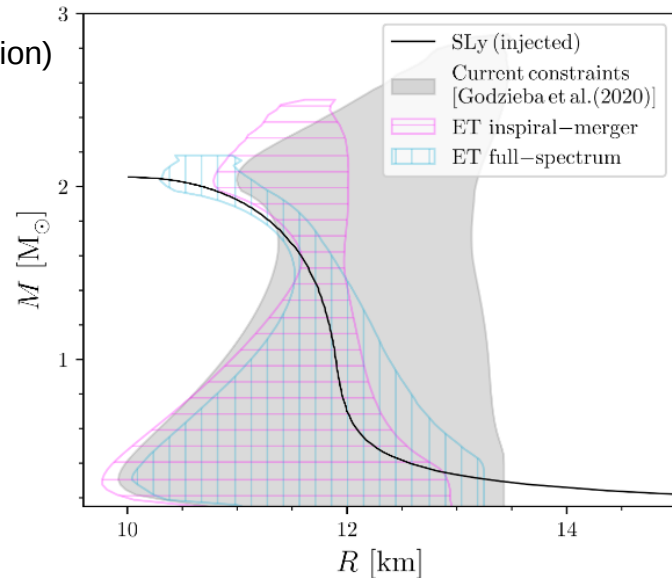
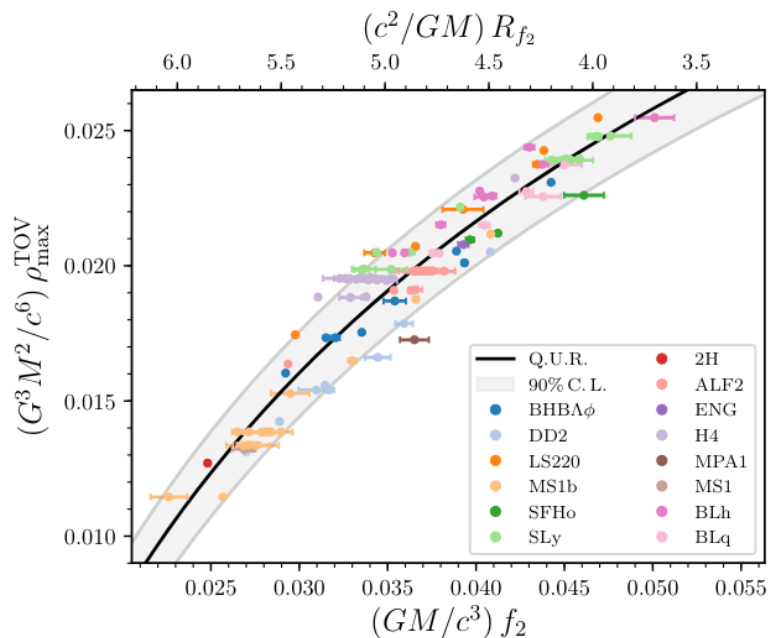


FIG. 4. Mass-radius diagram constraints from a single full-spectrum Einstein Telescope (ET) BNS observation with PM SNR 10 (total SNR 180). The gray area (prior) corresponds to the two-million EOS sample of Ref. [69]. The magenta and cyan areas are the 90% credibility regions given by inspiral-merger and inspiral-merger-PM inferences respectively. The full-spectrum (cyan) posterior agrees with the injected EOS (black).

Eccentricity

The strange case of GW190521

GW190521: A Binary Black Hole Merger with a Total Mass of $150 M_{\odot}$

R. Abbott *et al.*^{*}
(LIGO Scientific Collaboration and Virgo Collaboration)

Quasi-circular BBH, large in-plane spins

Highly eccentric BBH, large in-plane spins

GW190521 as a Highly Eccentric Black Hole Merger

V. Gayathri,¹ J. Healy,² J. Lange,² B. O'Brien,¹ M. Szczepańczyk,¹ I. Bartos,^{1,*} M. Campanelli,² S. Klimentko,¹ C. Lousto,² and R. O'Shaughnessy^{2,†}

**GW190521 as a merger of Proca stars:
a potential new vector boson of 8.7×10^{-13} eV**

Juan Calderón Bustillo,^{1,2,3,4,□} Nicolas Sanchis-Gual,^{5,6,□} Alejandro Torres-Forné,^{7,8,9} José A. Font,^{8,9} Avi Vajpeyi,^{3,4} Rory Smith,^{3,4} Carlos Herdeiro,⁶ Eugen Radu,⁶ and Samson H. W. Leong²

Head on collision of Proca stars

High mass ratio BBH ($q \sim 5-10$), plus large in-plane spins

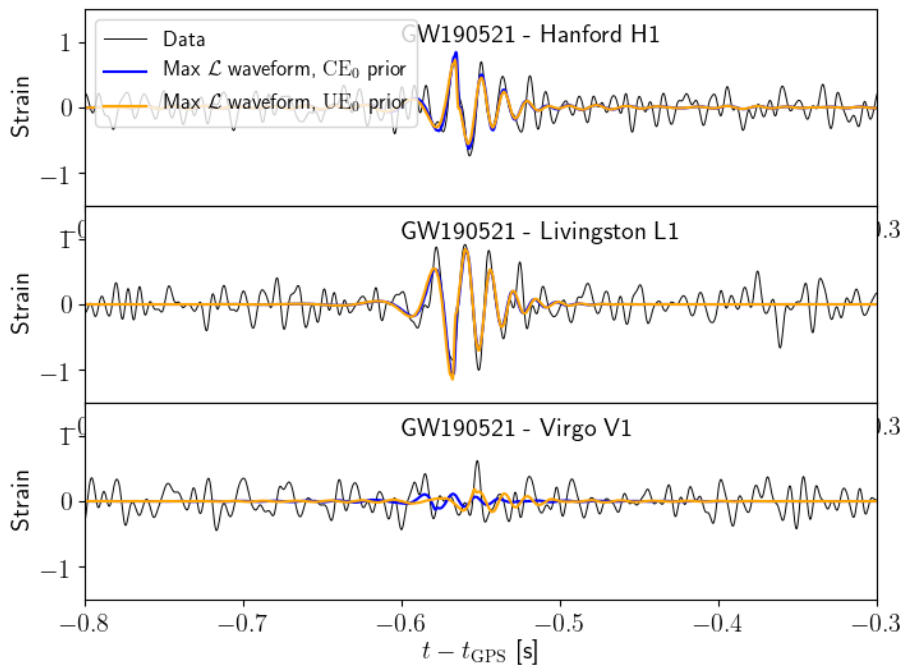
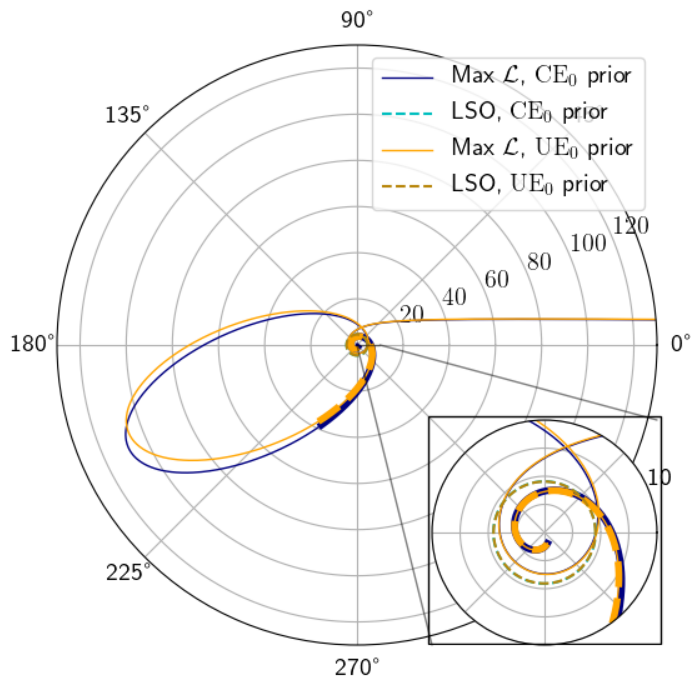
GW190521 may be an intermediate mass ratio inspiral

ALEXANDER H. NITZ^{1,2} AND COLLIN D. CAPANO^{1,2}

Hyperbolic merger: best fitting (maxL) dynamics and waveform

Consistent between the two energy priors employed

Gamba+ [<https://arxiv.org/abs/2106.05575>]



Results

Masses consistent with LVC

To reduce systematics, we also re-analyze the data using the preprocessing, quasi-circular NRSurr (and reproduce LVC results) and TEOBResumS

Waveform	TEOBResumS [19, 20]	TEOBResumS [19, 20]	NRSur7dq4 [36]	NRSur7dq4 [36]
E_0 prior	Unconstrained (UE_0)		Constrained (CE_0)	–
Multipoles	$(\ell, m) = (2, 2)$	$(\ell, m) = (2, 2)$	$(\ell, m) = (2, 2)$	$\ell \leq 4$
$m_1 [M_\odot]$	85^{+88}_{-22}	81^{+62}_{-25}	120^{+42}_{-34}	83^{+20}_{-14}
$m_2 [M_\odot]$	59^{+18}_{-37}	52^{+32}_{-32}	49^{+29}_{-22}	63^{+15}_{-15}
$M_{\text{source}} [M_\odot]$	151^{+73}_{-51}	130^{+75}_{-43}	171^{+27}_{-25}	146^{+24}_{-17}
$m_2/m_1 \leq 1$	$0.69^{+0.27}_{-0.52}$	$0.63^{+0.31}_{-0.43}$	$0.43^{+0.43}_{-0.25}$	$0.77^{+0.20}_{-0.28}$
χ_{eff}	–	–	$0.02^{+0.24}_{-0.27}$	$0.09^{+0.38}_{-0.25}$
χ_p	–	–	$0.78^{+0.17}_{-0.37}$	$0.66^{+0.27}_{-0.36}$
e	–	–	–	–
E^0/M	$1.014^{+0.009}_{-0.012}$	$1.014^{+0.010}_{-0.012}$	–	–
p_φ^0	$4.18^{+0.50}_{-0.62}$	$4.24^{+0.57}_{-0.37}$	–	–
SNR	$15.5^{+0.2}_{-0.3}$	$15.5^{+0.2}_{-0.2}$	$14.3^{+0.3}_{-0.4}$	$14.2^{+0.3}_{-0.3}$
$\log(\mathcal{L})_{\text{max}}$	120.215	119.282	106.058	104.371
$\log \mathcal{B}_{\text{noise}}^{\text{signal}}$	84.00 ± 0.18	83.30 ± 0.18	74.52 ± 0.16	73.25 ± 0.15

Capture scenario has higher SNR, evidence and higher likelihood than quasi-circular (or other published) analyses

TEOBResumS for generic orbits

Gravitational radiation reaction along general orbits in the effective one-body formalism

Donato Bini

Istituto per le Applicazioni del Calcolo “M. Picone,” CNR, I-00185 Rome, Italy

Thibault Damour

Institut des Hautes Études Scientifiques, F-91440 Bures-sur-Yvette, France

(Dated: September 11, 2018)

We derive the gravitational radiation-reaction force modifying the Effective One Body (EOB) description of the conservative dynamics of binary systems. Our result is applicable to general orbits (elliptic or hyperbolic) and keeps terms of fractional second post-Newtonian order (but does not include tail effects). Our derivation of radiation-reaction is based on a new way of requiring energy and angular momentum balance. We give several applications of our results, notably the value of the (minimal) “Schott” contribution to the energy, the radial component of the radiation-reaction force, and the radiative contribution to the angle of scattering during hyperbolic encounters. We present also new results about the conservative relativistic dynamics of hyperbolic motions.

Faithful analytical effective-one-body waveform model for spin-aligned, moderately eccentric, coalescing black hole binaries

Danilo Chiaramello^{1,2} and Alessandro Nagar^{2,3}

¹*Dipartimento di Fisica, Università di Torino, Via Pietro Giuria 1, 10125 Torino, Italy*

²*INFN Sezione di Torino, Via Pietro Giuria 1, 10125 Torino, Italy*

³*Institut des Hautes Etudes Scientifiques, 91440 Bures-sur-Yvette, France*

 (Received 31 January 2020; accepted 27 April 2020; published 26 May 2020)

$$\mathcal{F}_\varphi^{\text{EOB}_{\text{qc}}} = -\frac{32}{5}\nu^2 r_\omega^4 \Omega^5 \hat{f}(\Omega), \quad (6)$$

where $\Omega \equiv \dot{\varphi}$, which yields a more faithful representation of GW losses during the plunge [50, 51]. This expression is the leading quasi-circular term of the Newtonian angular momentum flux, obtained from Eq. (3.26) of Ref. [44], neglecting higher-order derivatives of (r, Ω) . We can thus improve Eq. (6) multiplying it with the Newtonian non-circular factor

$$\begin{aligned} \hat{f}_\varphi^{\text{Newt}_{\text{nc}}} = & 1 + \frac{3}{4} \frac{\ddot{r}^2}{r^2 \Omega^4} - \frac{\ddot{\Omega}}{4\Omega^3} + \frac{3\dot{r}\dot{\Omega}}{r\Omega^3} \\ & + \frac{4\dot{r}^2}{r^2 \Omega^2} + \frac{\ddot{\Omega}\dot{r}^2}{8r^2 \Omega^5} + \frac{3}{4} \frac{\dot{r}^3 \dot{\Omega}}{r^3 \Omega^5} + \frac{3}{4} \frac{\dot{r}^4}{r^4 \Omega^4} + \frac{3}{4} \frac{\dot{\Omega}^2}{\Omega^4} \\ & - \ddot{r} \left(\frac{\dot{r}}{2r^2 \Omega^4} + \frac{\dot{\Omega}}{8r\Omega^5} \right) + \ddot{r} \left(-\frac{2}{r\Omega^2} + \frac{\ddot{\Omega}}{8r\Omega^5} + \frac{3}{8} \frac{\dot{r}\dot{\Omega}}{r^2 \Omega^5} \right), \end{aligned} \quad (7)$$

in order to get

$$\mathcal{F}_\varphi^{\text{EOB}_{\text{Newt}_{\text{nc}}}} = -\frac{32}{5}\nu^2 r_\omega^4 \Omega^5 \hat{f}_\varphi^{\text{Newt}_{\text{nc}}} \hat{f}(\Omega). \quad (8)$$

$$\hat{\mathcal{F}}_r^{\text{NCN}} = \frac{32}{3}\nu \frac{p_{r^*}}{r^4} P_2^0 [\hat{f}_r^{\text{N}} + \hat{f}_r^{\text{1PN}} + \hat{f}_r^{\text{2PN}}],$$

Phenomenology: full GR prediction (w/ rad.react)

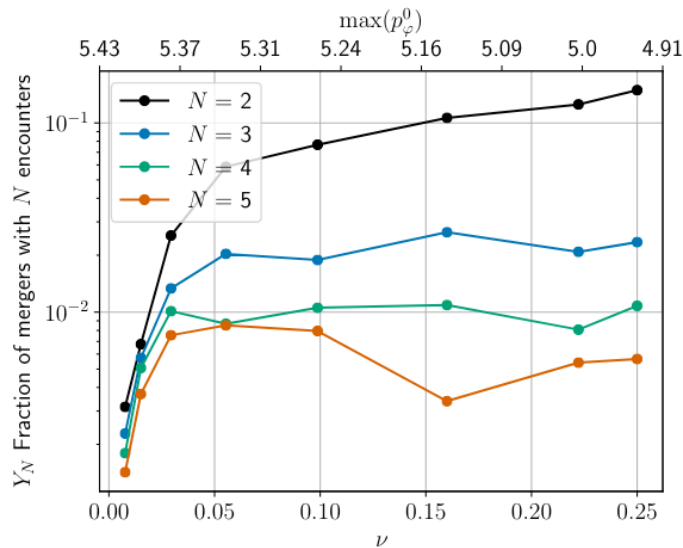
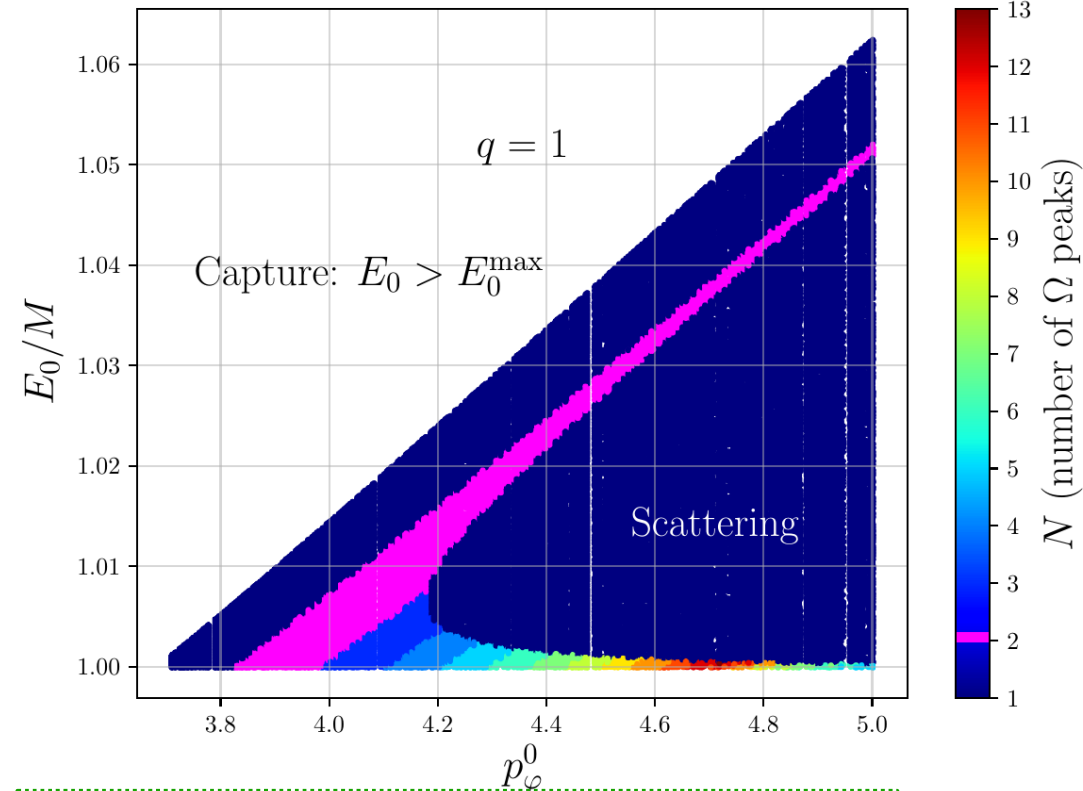


FIG. 5. Fraction of BBH configurations (including also scattering events) that end up with N encounters (where the N -th encounter corresponds to merger) for nonspinning binaries. Configurations with $N = 2$ are the most frequent ones, although their frequency quickly decreases below 10% as $q > 4$ ($\nu < 0.16$).

Effective-one-body waveforms from dynamical captures in black hole binaries

Alessandro Nagar^{1,2}, Piero Retteno^{1,3}, Rossella Gamba⁴, and Sebastiano Bernuzzi⁴

¹ INFN Sezione di Torino, Via P. Giuria 1, 10125 Torino, Italy

² Institut des Hautes Etudes Scientifiques, 91440 Bures-sur-Yvette, France

³ Dipartimento di Fisica, Università di Torino, via P. Giuria 1, 10125 Torino, Italy and

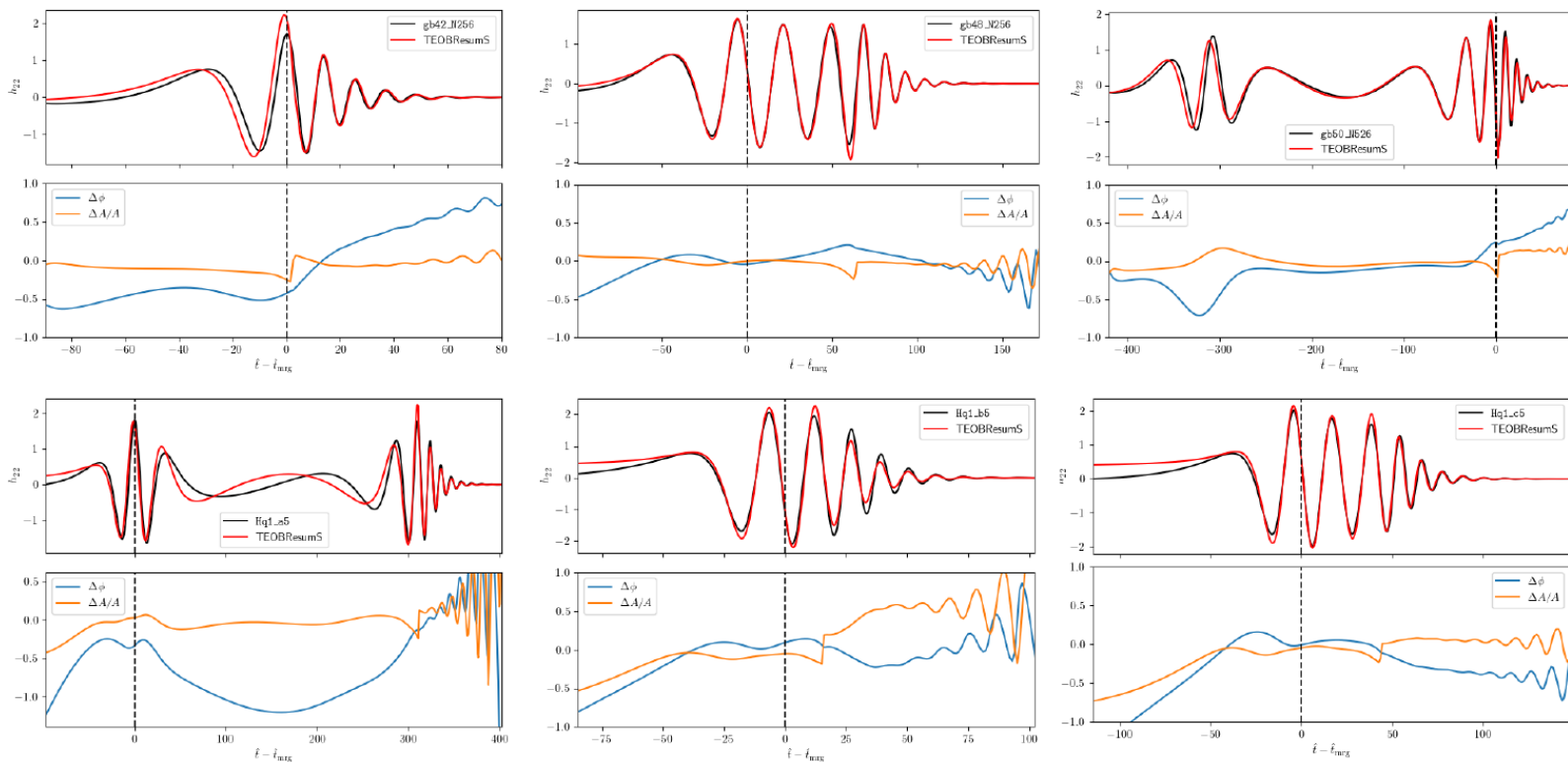
⁴ Theoretisch-Physikalisches Institut, Friedrich-Schiller-Universität Jena, 07743, Jena, Germany

(Dated: October 1, 2020)

[<https://arxiv.org/abs/2009.12857>]

Validation: numerical relativity comparisons

Preliminary



NR simulations performed with [GR Athena++](#)

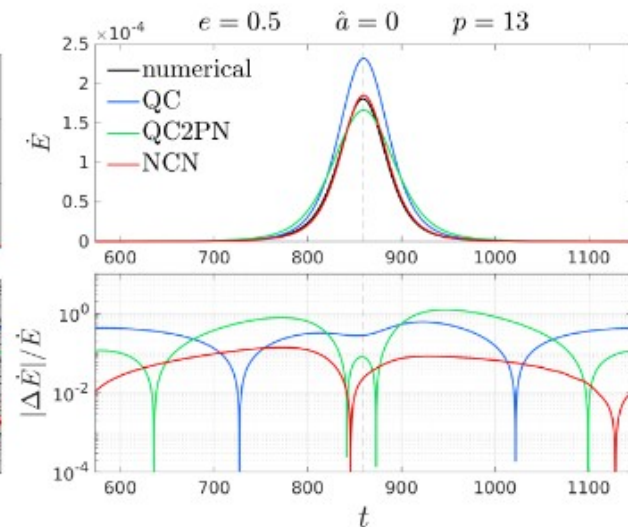
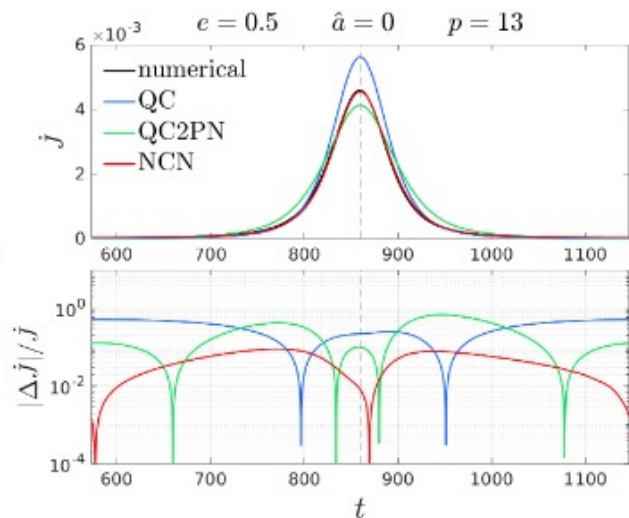
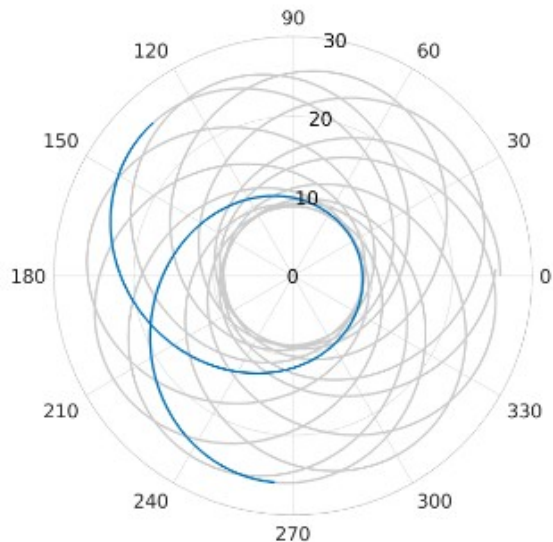
+ < 1(3) % matches against RIT catalog

Comparing prescriptions for rad.react.

NCN: Noncircular multiplicative/resummed correction to Newtonian prefactor +Fr P02

QC: Quasicircular +Fr [Ramos-Buades+ <https://arxiv.org/abs/2112.06952>]

QC2PN: QC *times* 2PN noncircular corrections [Khalil+ <https://arxiv.org/abs/2104.11705>]



Albanesi+ [<https://arxiv.org/abs/2202.10063>]

Placidi+ [<https://arxiv.org/abs/2112.05448>] \rightarrow NCN2PN

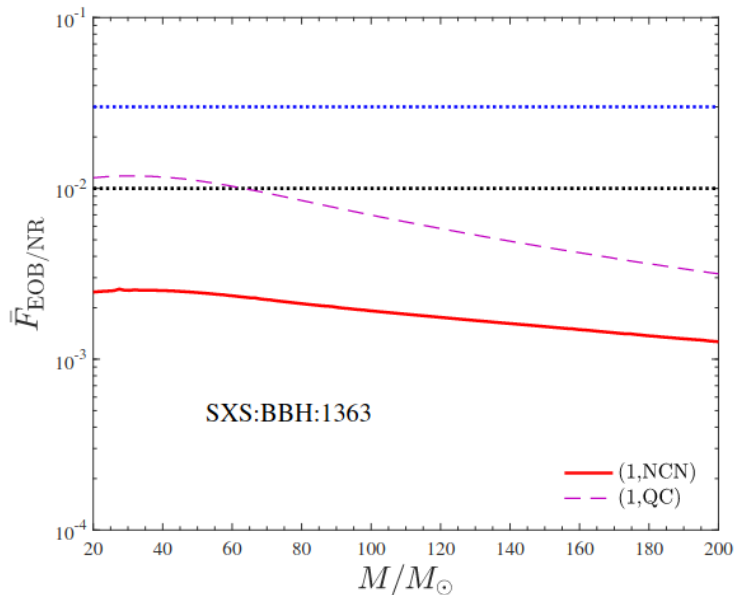


FIG. 10. EOB/NR unfaithfulness computation with the Advanced LIGO noise using the standard NCN `TEOBResumS` model of Ref. [21] or the QC version discussed here. The faster circularization of the QC model results in $\bar{F}_{\text{EOB/NR}}$ slightly above the 1% threshold (see Fig. [11]).

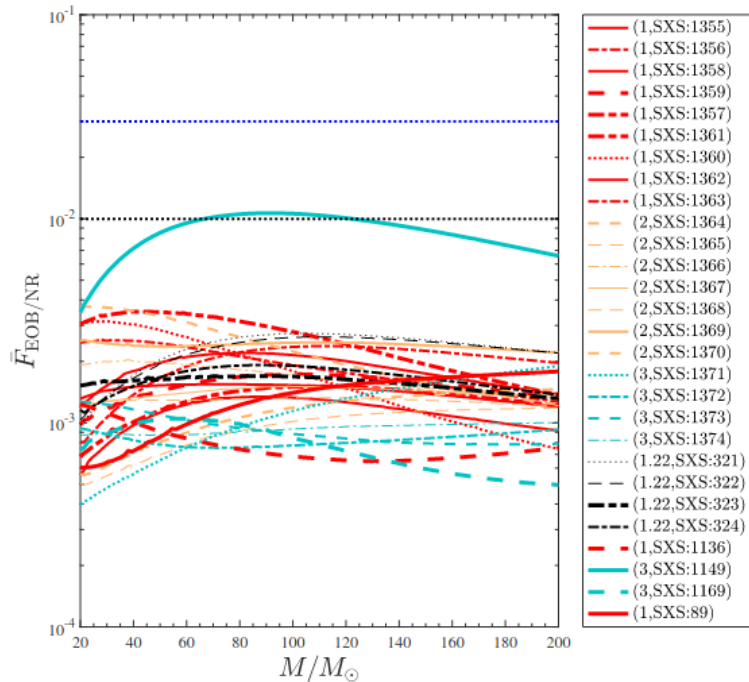


FIG. 14. EOB/NR unfaithfulness for the $\ell = m = 2$ mode computed over the eccentric SXS simulations publicly available, Table [IV]. The horizontal lines mark the 0.03 and 0.01 values. The value of $\bar{F}_{\text{EOB/NR}}^{\text{max}}$ does not exceed the 0.7% except for the single outlier given by SXS:BBH:1149, corresponding to $(3, +0.70, +0.60)$ with $e_{\omega_a}^{\text{NR}} = 0.037$, that is around 1%. This is consistent with the slight degradation of the model performance for large positive spins already found in the quasi-circular limit, as pointed out in Ref. [25].

BBH scattering: NR/AR comparison

PHYSICAL REVIEW D **89**, 081503(R) (2014)

Strong-field scattering of two black holes: Numerics versus analytics

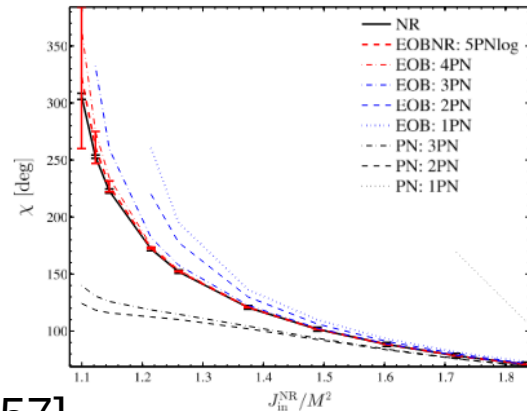
Thibault Damour,¹ Federico Guercilena,^{2,3} Ian Hinder,² Seth Hopper,² Alessandro Nagar,¹ and Luciano Rezzolla^{3,2}

¹*Institut des Hautes Etudes Scientifiques, 91440 Bures-sur-Yvette, France*

²*Max-Planck-Institut für Gravitationsphysik, Albert-Einstein-Institut,
Am Mühlenberg 1, D-14476 Golm, Germany*

³*Institut für Theoretische Physik, Max-von-Laue-Str. 1, D-60438 Frankfurt am Main, Germany*

(Received 28 February 2014; published 8 April 2014)



Nagar, Retegno, Gamba, SB [<https://arxiv.org/abs/2009.12857>]

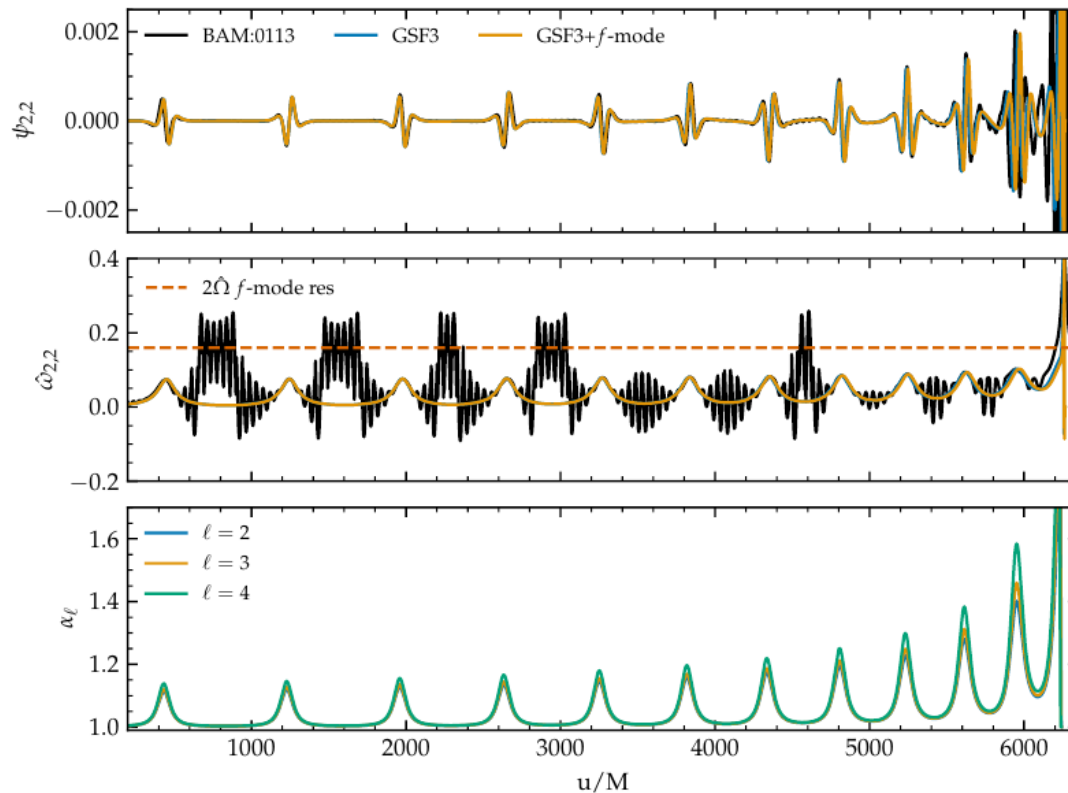
TABLE I. EOB scattering angle and comparison with the NR data of Ref. [15]. These results correspond to the standard configuration of the model, i.e. with 3PN-accurate D and Q functions. From left to right, the columns report: the configuration number; the minimum of the EOB radial separation (EOB impact parameter); the initial energy \hat{E}^0 and angular momentum p_φ^0 ; the NR and EOB energy losses; the NR and EOB angular momentum losses; the NR and EOB scattering angles and their fractional difference $\hat{\Delta}\chi^{\text{NREOB}} \equiv |\chi^{\text{NR}} - \chi^{\text{EOB}}|/\chi^{\text{NR}}$. Angles are measured in degrees. Note that, within the EOB, configuration #1 does not scatter, but plunges instead.

#	r_{\min}	\hat{E}^0	p_φ^0	$\Delta E^{\text{NR}}/M$	$\Delta E^{\text{EOB}}/M$	$\Delta J^{\text{NR}}/M^2$	$\Delta J^{\text{EOB}}/M^2$	χ^{NR}	χ^{EOB}	$\hat{\Delta}\chi^{\text{NREOB}}[\%]$
1	...	1.0225555(50)	4.3986080	0.01946(17)	0.032553	0.17007(89)	0.363750	305.8 (2.6)
2	3.70	1.0225722(50)	4.49039348	0.01407(10)	0.014083	0.1380(14)	0.134495	253.0(1.4)	279.35	10.4
3	4.03	1.0225791(50)	4.58209352	0.010734(75)	0.00951037	0.1164(14)	0.101919	222.9(1.7)	234.22	5.1
4	4.85	1.0225870(50)	4.8570920	0.005644(38)	0.0041582	0.076920(80)	0.0588254	172.0(1.4)	174.23	1.3
5	5.34	1.0225870(50)	5.0403920	0.003995(27)	0.00272826	0.06163(53)	0.045189	152.0(1.3)	153.01	0.7
6	6.49	1.0225884(50)	5.4986320	0.001980(13)	0.001172	0.04022(53)	0.027481	120.7(1.5)	120.79	0.07
7	7.59	1.0225924(50)	5.9568680	0.0011337(90)	0.0005951	0.029533(53)	0.018992	101.6(1.7)	101.51	0.09
8	8.66	1.0225931(50)	6.4150960	0.007108(77)	0.000332568	0.02325(47)	0.0141277	88.3(1.8)	88.19	0.12
9	9.72	1.0225938(50)	6.8733240	0.0004753(75)	0.00019778	0.01914(76)	0.0110359	78.4(1.8)	78.28	0.15
10	10.78	1.0225932(50)	7.33153432	0.0003338(77)	0.0001226	0.0162(11)	0.008928	70.7(1.9)	70.54	0.23

More...

Highly eccentric BNS encounters

Preliminary
Gamba, SB



NR simulations: Stephens+ (BHNS) [<https://arxiv.org/abs/1105.3175>]

Gold, SB+ [<https://arxiv.org/abs/1109.5128>] Chaurasia+ [<https://arxiv.org/abs/2003.11901>]

Intermediate mass-ratio regime

Numerical-relativity validation of effective-one-body waveforms
in the intermediate-mass-ratio regime

Alessandro Nagar^{1,2}, James Healy³, Carlos O. Lousto³, Sebastiano Bernuzzi⁴, and Angelica Albertini^{5,6}

¹INFN Sezione di Torino, Via P. Giuria 1, 10125 Torino, Italy

²Institut des Hautes Etudes Scientifiques, 91440 Bures-sur-Yvette, France

³Center for Computational Relativity and Gravitation,

School of Mathematical Sciences, Rochester Institute of Technology,

85 Lomb Memorial Drive, Rochester, New York 14623, USA

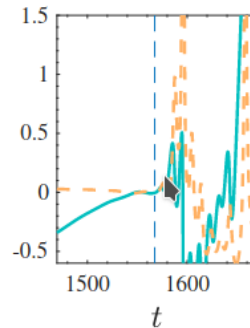
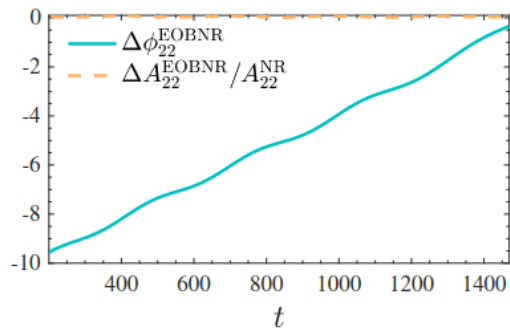
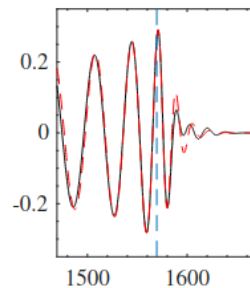
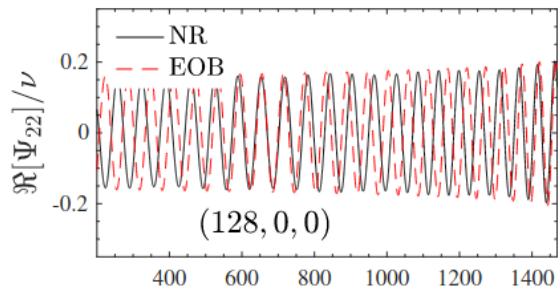
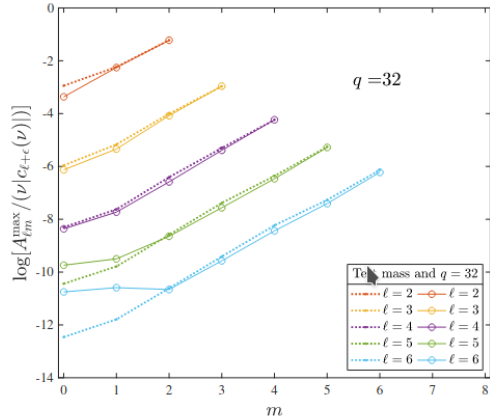
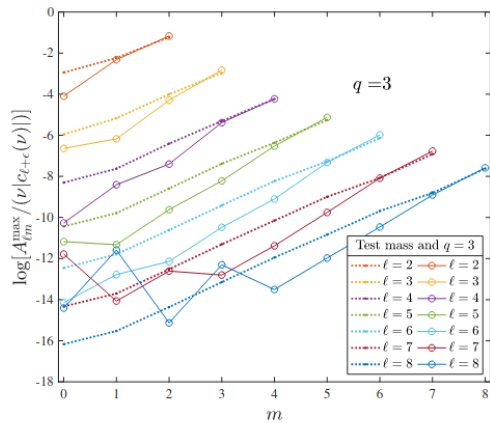
Theoretisch-Physikalisches Institut, Friedrich-Schiller-Universität Jena, 07743, Jena, Germany

⁵Astronomical Institute of the Czech Academy of Sciences,

Boční II 1401/1a, CZ-141 00 Prague, Czech Republic and

⁶Faculty of Mathematics and Physics, Charles University in Prague, 18000 Prague, Czech Republic

(Dated: February 14, 2022)



Towards 3G

Albertini+ [<https://arxiv.org/abs/2111.14149>]

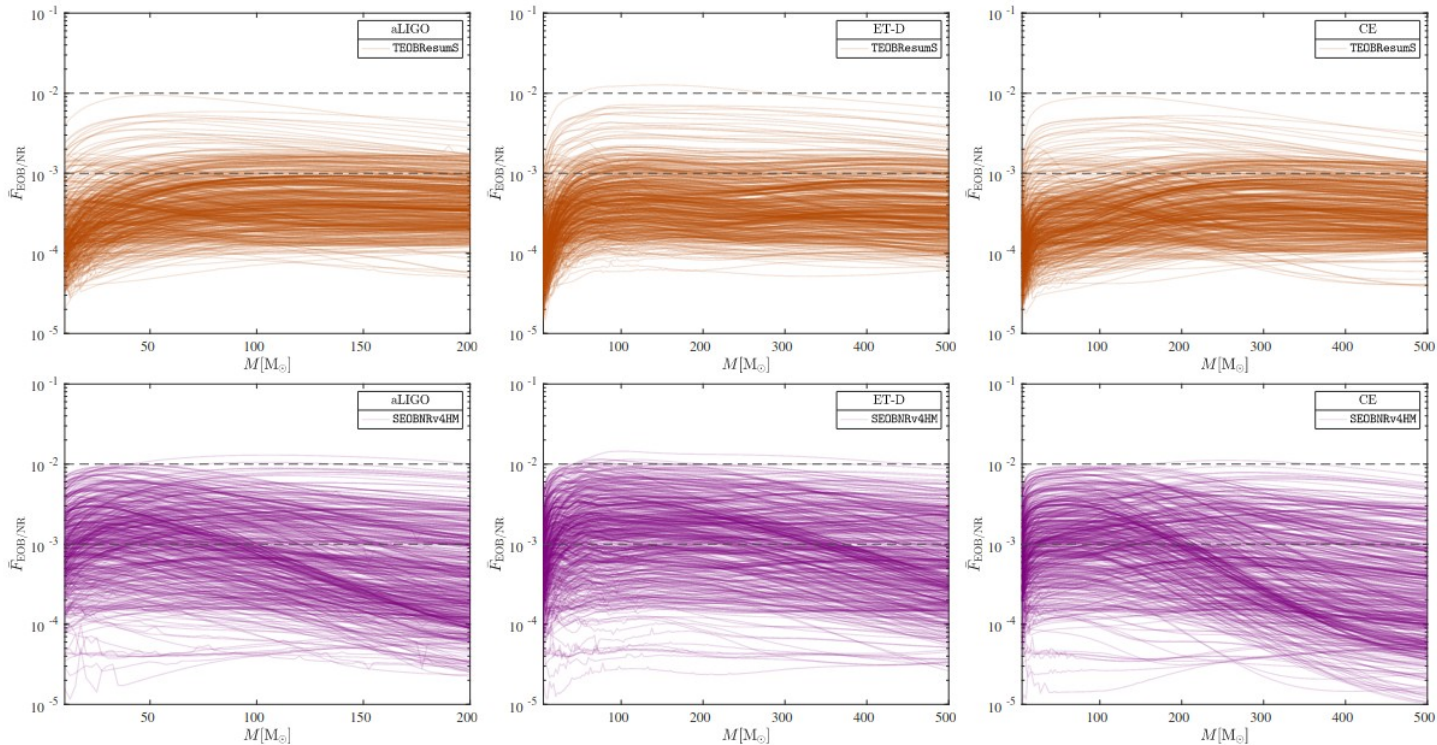
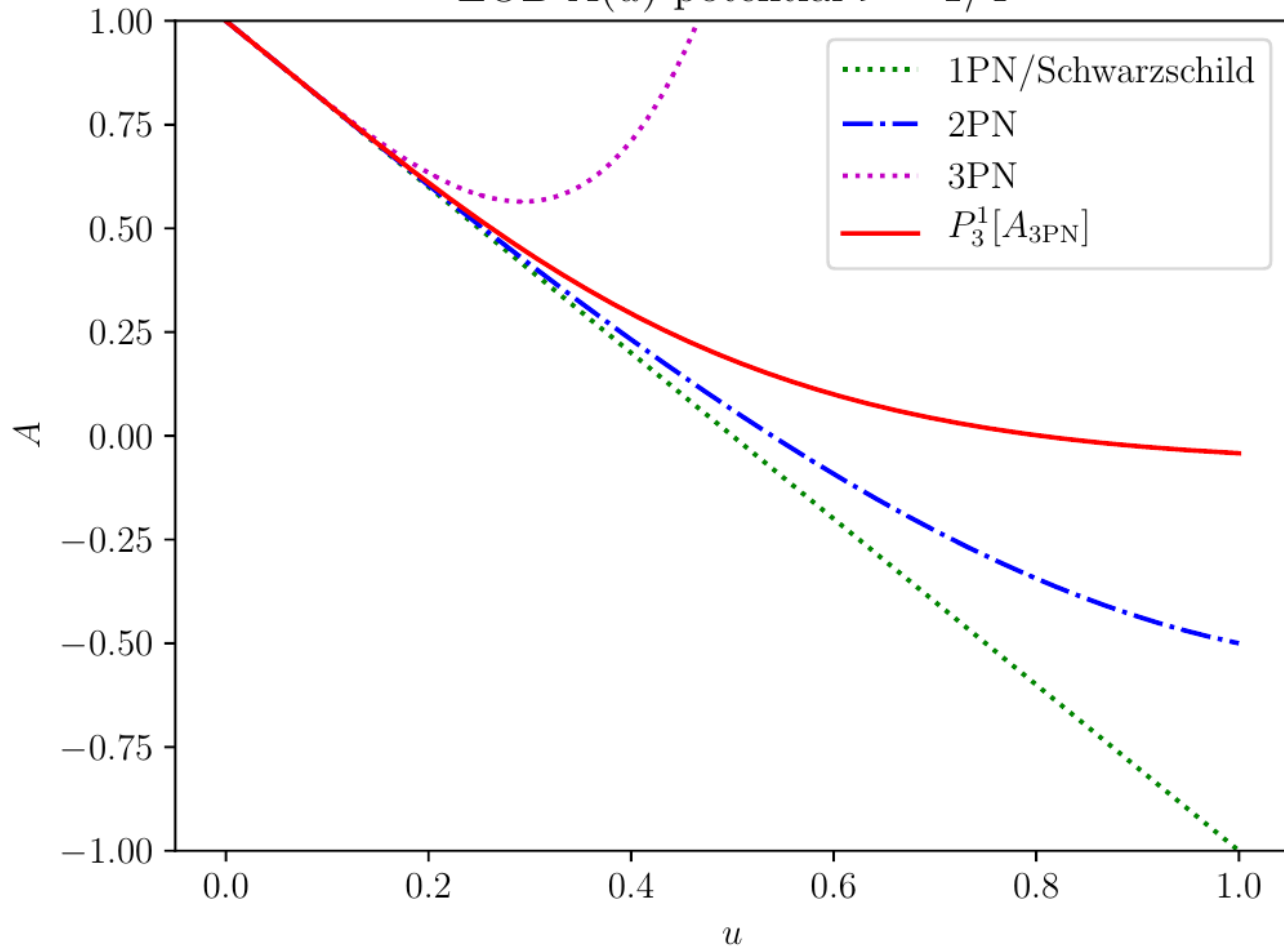


FIG. 18. Direct EOB/NR unfaithfulness comparison using the standard implementation of `TEOBResumS` (top panels) and `SEOBNRv4HM` (bottom panels). Again, the unfaithfulness is evaluated for the sample of 534 nonprecessing quasicircular NR simulations of the SXS catalog (likewise Fig. 12) using: (i) the zero-detuned, high-power noise spectral density of Advanced LIGO (first column), (ii) the expected PSD for Einstein Telescope (second column), (iii) the expected PSD for Cosmic Explorer (third column).

Summary & thanks!

- Today
 - Tidal effects:
 - Further advances likely require more accurate NR simulations
 - Eccentricity and generic orbits:
 - Robust framework to be improved with upcoming analytical results
- Last weeks
 - GR 2-body problem is rich and historically benefitted of various approaches
 - e.g. the EOB map comes from “thinking quantum mechanically”
 - Looking forward for more information ...
 - ... do not lose the big picture: PN/PM/GSF/NR/etc results must be incorporated into a coherent framework! (“resum”)

Backup slides

EOB $A(u)$ potential $\nu = 1/4$ 

Improved resummation of post-Newtonian multipolar waveforms from circularized compact binaries

Thibault Damour,^{1,2} Bala R. Iyer,^{1,3} and Alessandro Nagar^{1,2,4}

¹*Institut des Hautes Etudes Scientifiques, 91440 Bures-sur-Yvette, France*

²*ICRANet, 65122 Pescara, Italy*

³*Raman Research Institute, Bangalore 560 080, India*

⁴*INFN, Sezione di Torino, Via Pietro Giuria 1, Torino, Italy*

(Received 13 November 2008; published 3 March 2009)

The structure of this Hamiltonian can be clarified by introducing the (gauge-invariant) concept of “centrifugal radius” $r_c(r)$, defined so that the orbital part of the Hamiltonian ruling equatorial orbits ($\theta = \pi/2$) can be written as

$$H_{\text{orb,eq}}^{\text{Kerr}}(r; p_r, p_\varphi) = \sqrt{A^{\text{eq}}(r) \left(\mu^2 + \frac{p_\varphi^2}{r_c^2} + \frac{p_r^2}{B^{\text{eq}}(r)} \right)}, \quad (8)$$

with the usual, relativistic centrifugal energy term $\mu^2 + p_\varphi^2/r_c^2$. By comparing with Eq. (2) one obtains

$$r_c^2 \equiv \frac{\mathcal{R}^4(r)}{r^2} = r^2 + a^2 + \frac{2Ma^2}{r}. \quad (9)$$

As indicated above, the resummation method we shall use here consists in: (i) decomposing the PN-correction factor $\hat{h}_{\ell m}^{(\epsilon)} = 1 + h_1 x + h_{1.5} x^{3/2} + \dots$ into the *product of four factors*, each of which has a similar PN expansion, $1 + \mathcal{O}(x)$, namely

$$\hat{h}_{\ell m}^{(\epsilon)} = \hat{S}_{\text{eff}}^{(\epsilon)} T_{\ell m} e^{i\delta_{\ell m}} \rho_{\ell m}^\ell, \quad (8)$$

and then (ii), resumming separately each factor.

New effective-one-body description of coalescing nonprecessing spinning black-hole binaries

Thibault Damour and Alessandro Nagar

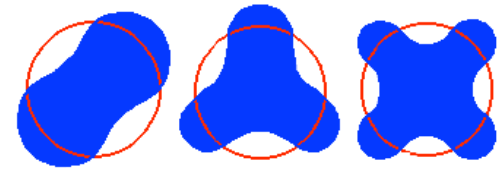
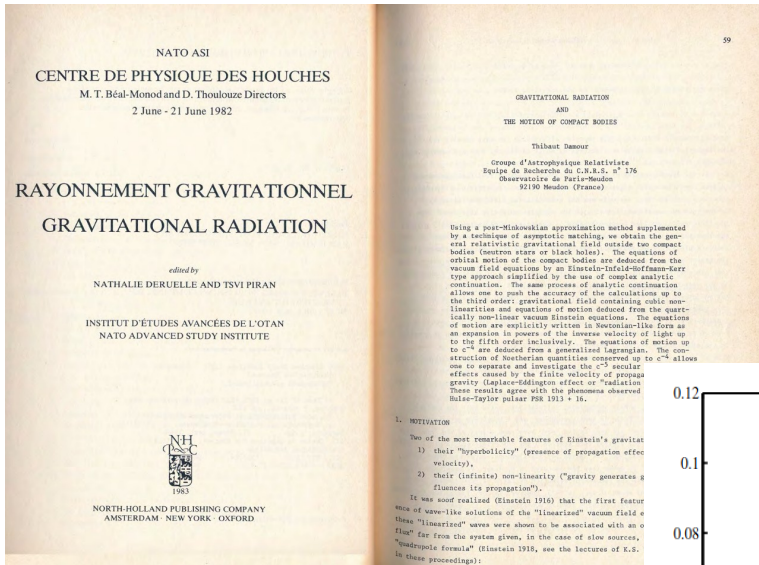
Institut des Hautes Etudes Scientifiques, 91440 Bures-sur-Yvette, France

(Received 26 June 2014; published 13 August 2014)

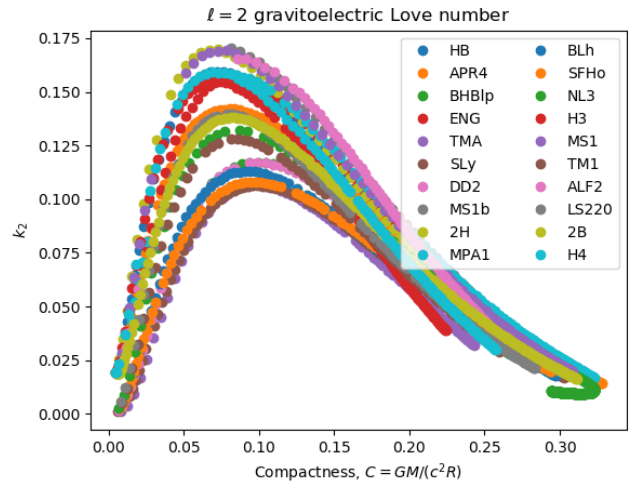
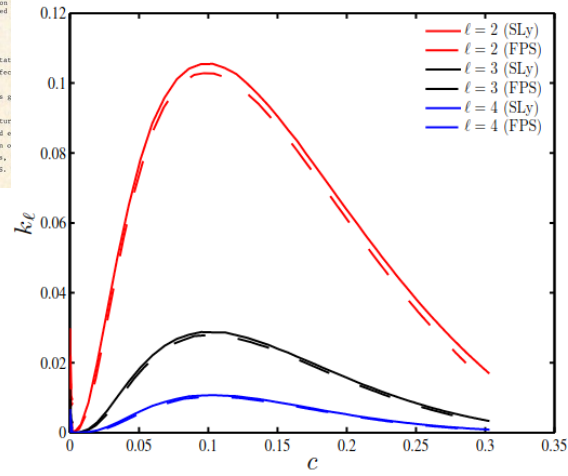
$$r_c^2 = r^2 + \tilde{a}_Q^2 \left(1 + \frac{2}{r} \right) + \frac{\delta a_{\text{NLO}}^2}{r} + \frac{\delta a_{\text{NNLO}}^2}{r^2} + \frac{\delta a_{\text{LO}}^4}{r^2}. \quad (25)$$

Love numbers depends on EOS and NS compactness

“inner problem”



$$Q_{ij} = \lambda_2 G_{ij} \sim \lambda_2 \partial_i \partial_j \phi$$



PHYSICAL REVIEW D **80**, 084035 (2009)
Relativistic tidal properties of neutron stars
 Thibault Damour^{1,2} and Alessandro Nagar^{1,2}
¹Institut des Hautes Etudes Scientifiques, 91440 Bures-sur-Yvette, France
²ICRANet, 65122 Pescara, Italy
 (Received 30 May 2009; published 23 October 2009)

See also Hinderer 2007, Binnington&Poisson 2009

3. DIGEST OF THE HISTORY OF THE PROBLEM OF MOTION

In 1687, I. Newton showed how the orbital motion of approximately spherical extended objects could be well-approximated by the motion of point masses. This is a very important result of Newtonian physics whose extension to General Relativity is highly non-trivial, as was pointed out by M. Brillouin (1922). M. Brillouin called this schematization of an extended body by a point mass with disappearance of all internal structure: "le principe d'effacement" ("effacing principle;" perhaps a more picturesque name would be: "the Cheshire cat principle"). In Newtonian physics the proof of this "effacing principle" makes an essential use of:

- 1) the linearity of the gravitational field as a function of the matter distribution (which allows one to define and separate the self-field and the external field);
- 2) the Action and Reaction principle (which allows one to define the center of mass and to ignore the contribution of the self-field to its motion);
- 3) Newton's theorem on the attraction of spherical bodies.

More specifically, for a binary system constituted of non-rotating nearly spherical bodies of masses m and m' , one deduces from 1) that the main correction to the point mass idealization will come from the tidal field $Gm'd^{-3}r$ (where G is Newton's constant, r is the distance away from the center of mass of the first object m , and d is the distance between the two objects). If b denotes the radius of the first object, the tidal field will deform slightly its shape:

$\delta b/b = h(m'/d^3)(b^3/m)$, where h , the first Love (1909) number, is a dimensionless quantity of order unity. This deformation induces in turn a small quadrupole moment: $Q = k m'b^5d^{-3}$, where k , the second Love number, is a dimensionless quantity of order unity ($h = 3/5$ and $k = 4/15$ for the Earth). Finally this tidally induced quadrupole moment will create a small correction to Newton's law for point masses: $\delta F/F \sim k (b/d)^5$. Therefore as long as the radii of the objects are much smaller than their mutual distances, their internal structure (if they are not rotating) will be utterly negligible. We shall show in Section 5 how this result of "effacing" can be extended to Einstein's theory even, and in fact most accurately, in the case of compact objects, i.e. when the radius $b \sim Gm/c^2$. But as we shall not be able to use 1) and 2) above, we shall need a completely different approach to show that the very strong "self field" of the compact object does not contribute to its orbital motion.

Then one can find in vacuum a decoupled second order differential equation for $H = H_0 = H_2$ for instance (Edelstein and Vishveshwara 1970, Demianski and Grishchuk 1974):

$$\hat{R}(\hat{R}-2)d^2(H/\hat{R}(\hat{R}-2))/d\hat{R}^2 + 3(2\hat{R}-2)d(H/\hat{R}(\hat{R}-2))/d\hat{R} - (L-2)(L+3)H/\hat{R}(\hat{R}-2) = 0. \quad (10)$$

The general solution of this second order differential equation contains 2 arbitrary constants. For instance, when $L = 2$, one finds for the general quadrupolar H perturbation in vacuum, i.e. outside the body:

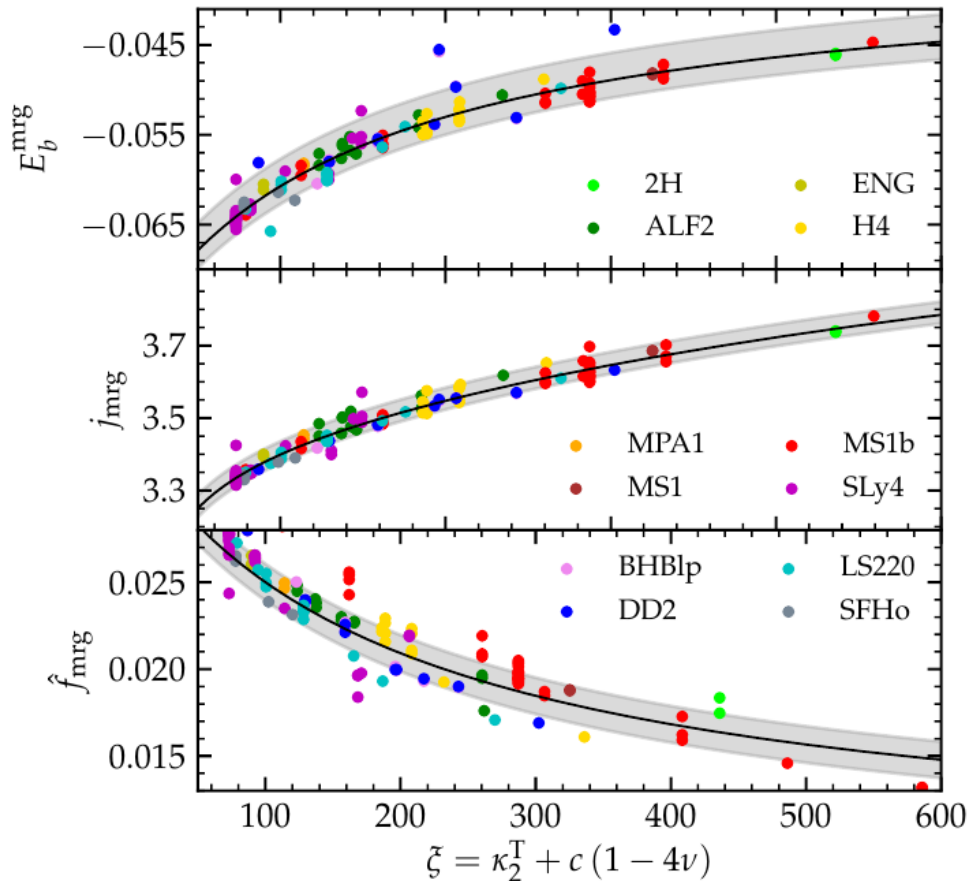
$$H = D(\hat{R}(\hat{R}-2) + k \hat{R}(\hat{R}-2) \int_{\hat{R}}^{\infty} 5dx/(x^3(x-2)^3)). \quad (11)$$

The dimensionless constant k is a relativistic generalization (Damour 1981) of the second Love number (Love 1909) which was introduced in Section 3. It is, in a sense, a dimensionless measure of the yielding of the object to an external tidal solicitation. It depends on the internal structure of the body (equations of state,...) and can be determined for an ordinary body (not a black hole) by imposing the regularity of the metric perturbation H, K, h_0 at the center of the body and when crossing the surface of the body (see e.g., Thorne and Campolattaro 1967). By our hypothesis 1) we have $\hat{R} \sim 1$ at the radius of the object, therefore as there are no other scales in the problem, k must be of order unity (like the non-relativistic one):

$$k \sim 1 \quad (12)$$

(More generally for non-necessarily compact objects of dimensionless radius \hat{b} , one will have $k \sim \hat{b}^5$ which allows one to justify the remark after hypothesis 1)). In the case of a black hole, k is determined by imposing the regularity of metric perturbation on the future horizon: in this case one finds $k = 0$ (in agreement with D'Eath 1975a). Incidentally, one should not conclude from this result that there are no tidal responses of a black hole to an external solicitation: such a non-zero response is contained in the first term of the righthand side of (11): $\hat{R}(\hat{R}-2)$ which differs from the usual term (in absence of any object): \hat{R}^2 .

Merger parametrization (aka quasiuniversality)



- **How to interpret numerical-relativity (NR) data?**
- *Y-axis*: simulation results from multi-orbit NR simulations with different EOS, masses, mass-ratio, spins, etc.
- *X-axis*: tidal coupling constant (plus effective correction for very asymmetric binaries)
- **Tidal coupling constant captures strong-field features to high precision!**
SB+ (2014) [<https://arxiv.org/abs/1402.6244>]
- **Why useful?**
 - Lower bounds for energy, angular momentum, radiated to merger (at the end of chirp)
 - GW merger frequency/amplitude (not predicted by post-Newtonian methods)
 - Peak luminosity and upper bounds for remnant's energy, ang.momentum, etc. [Zappa, SB+ (2017)]